from **Astrophysical Implications of the Laboratory Study of Presolar Materials,** edited by T. J. Bernatowicz and E. Zinner, AIP CP402, 1997, pp.59–82

Presolar Oxide Grains in Meteorites

Larry R. Nittler

Department of Terrestrial Magnetism, Carnegie Institution of Washington, 5241 Broad Branch Road NW, Washington, D. C. 20015, USA

Abstract.

Ninety-two refractory oxide grains (primarily Al_2O_3) with highly unusual O-isotopic ratios have been found in acid-resistant residues of five primitive meteorites. Thirty-five of these also have large excesses of ^{26}Mg, attributable to the *in situ* decay of radioactive ^{26}Al. The extreme ranges of isotopic compositions of the grains indicate that they are unprocessed stellar condensates. The grains have been divided into four groups. Group 1 grains have ^{17}O excesses and moderate ^{18}O depletions, relative to solar, and most likely formed around red giants and asymptotic giant branch (AGB) stars. However, many individual stars with different masses and initial compositions are required to explain the range of O-isotopic ratios and inferred ^{26}Al/^{27}Al ratios observed in the grains. Group 3 grains, which have ^{17}O and ^{18}O depletions, probably originated in O-rich red giants of very low mass ($M \lesssim 1.4 M_\odot$) and low metallicity. The Group 3 grains' compositions are probably strongly influenced by the chemical evolution of the Galaxy; they also provide a new method of determining the age of our Galaxy. Group 2 grains have large ^{18}O depletions, ^{17}O enrichments and high inferred ^{26}Al/^{27}Al ratios; they probably formed in low-mass AGB stars in which extra mixing ("cool bottom processing") occurred. The four Group 4 grains have ^{18}O enrichments. Possible explanations for these excesses include dredge-up of this isotope in early thermal pulses in AGB stars or an origin in low-mass red giants of unusually high metallicity. One grain, T54, is extremely enriched in ^{17}O and depleted in ^{18}O, and may have formed in an AGB star undergoing hot-bottom-burning. Presolar oxides are underabundant in meteorites, relative to presolar SiC, perhaps because Al condenses more readily into silicates than into refractory oxides or because presolar Al_2O_3 has a finer grain size distribution. No presolar oxide grains from supernovae have been identified, despite expectations that they should be present.

I INTRODUCTION

Primitive meteorites contain tiny grains of stardust: unprocessed specks of dust grains that condensed in stellar winds and/or explosions and were part of the protosolar cloud from which the Sun formed. These grains are recognized by their highly unusual isotopic ratios, the ranges of which far exceed those observed in material of Solar System origin. Since the first isolation of presolar diamonds, SiC and graphite

(1–3), most studies of stardust in meteorites have focused on C-rich phases rather than O-rich ones. This does not mean that O-rich stardust is scarce in the Galaxy. Rather, it reflects the fact that primitive meteorites are essentially collections of O-rich phases that formed in the early Solar System. Isotopically anomalous presolar oxide grains that survived Solar System formation are thus hidden by a large background of isotopically normal dust grains. This is true even in the highly concentrated acid residues in which presolar C-rich phases are prevalent. Nevertheless, since O-rich dust and C-rich dust form under different conditions, and since most of the dust in the Galaxy is believed to be O-rich, presolar oxides provide unique astrophysical information and are well worth the extra effort required to find them.

The first evidence for presolar oxide grains in a meteoritic acid residue was found by Zinner and Tang (4), who measured ^{17}O enrichments in bulk measurements of thousands of tiny (0.1–0.2 μm) oxide grains in a separate of the Murray carbonaceous chondrite. Subsequently, Huss *et al.* (5) reported the discovery of a highly ^{26}Mg-enriched corundum (Al_2O_3) grain from the Orgueil meteorite, out of fifty-one refractory oxide grains individually analyzed for Mg and Al. The inferred initial ^{26}Al/^{27}Al ratio of this grain is much higher than the upper limit of 5×10^{-5} observed in matter of Solar System origin (6), and Huss *et al.* tentatively identified this grain as presolar, an identification later confirmed by O-isotopic analysis (7).

Contemporary with the work of Huss and his coworkers at Caltech, an ion imaging system was developed for the Washington University ion microprobe, partly with the aim of efficiently locating isotopically highly anomalous presolar oxide grains. Using this system, low-precision ^{16}O/^{18}O ratios of large numbers of grains may be rapidly obtained and anomalous grains automatically identified for further study (see refs. (8,9) for detailed descriptions of the ion image mapping technique). The initial use of this ion imaging method resulted in the first unambiguous discovery of a presolar Al_2O_3 grain, in a residue of the Murchison meteorite (10). To date, a total of 92 presolar oxide grains have been found—eighty-nine corundums, one spinel ($MgAl_2O_4$), and two grains with compositions intermediate between corundum and spinel—in acid residues of five meteorites. The meteorites involved are listed in Table 1, along with the method used to find the grains (ion imaging or standard grain-by-grain analysis) and estimated concentrations. The grains are all

TABLE 1. The meteorites from which presolar oxide grains have been isolated. The third column indicates how grains were located: S=Single grain analysis; I=Ion imaging

Meteorite (Type)	Number	Method	Concentration (ppb)	References
Orgueil (CI)	2	S	10	(5,7,11)
Murchison (CM)	1	I	3	(10)
Bishunpur (LL)	3	S	5	(12,13)
Tieschitz (H)	83	I(75) S(8)	30	(8,9,14)
Acfer 094 (C)	3	I	3	(15)

0.5–4 μm in diameter. Most of the grains were found by ion imaging in a separate of the Tieschitz ordinary chondrite. Although ninety-two grains is a far cry from the several thousand individual SiC grains that have now been individually analyzed, even this limited data set has provided important astrophysical information not obtained from other presolar phases. This paper discusses the isotopic compositions and astrophysical implications of the presolar oxide grains, with emphasis both on the new information the grains can give us and on important outstanding problems associated with the data. For more details on topics discussed here, the reader is referred to two recent papers (9,16).

II ISOTOPIC COMPOSITIONS

With the exception of Orgueil-B, all of the known presolar oxide grains were identified by their anomalous O-isotopic ratios. The $^{16}O/^{17}O$ and $^{16}O/^{18}O$ ratios of the grains are shown in Fig. 1, together with the ratios measured spectroscopically in red giant and asymptotic giant branch (AGB) stars (17–22). These data are not truly representative of the population of presolar oxides in the parent meteorites. This is because grains with unusual $^{16}O/^{17}O$ ratios, but $^{16}O/^{18}O$ ratios close to the solar value of 499 ($^{16}O/^{18}O\sim$440-570), are missed by the ion imaging technique used to find most of the grains. Ion probe analyses of 400 single oxide grains indicated that some 25–50% of the presolar oxide grains in the meteoritic residues have been missed by ion imaging searches (9). However, the grains that are missed belong to the largest and best-understood group of presolar oxides (Group 1, see below).

The presolar grains have been divided into four groups on the basis of their O-isotopic ratios (8,14); the isotopic properties of the groups are summarized in Table 2. One grain, T54, does not appear to be related to any of the other groups, and is thus listed separately. Note that the boundaries between groups are not sharp and the assignment of a particular grain to a particular group is not always unambiguous. In particular, Groups 1, 2 and 3 all merge together in the region of $^{16}O/^{17}O>1000$, $500<^{16}O/^{18}O<1000$, and grains which lie in this area of the plot

TABLE 2. The characteristics of the four groups of presolar oxide grains and the unique grain T54

Group	Number	$^{16}O/^{17}O$	$^{16}O/^{18}O$	Fraction with ^{26}Al	$^{26}Al/^{27}Al$ Range	$^{26}Al/^{27}Al$ Mean
Solar		2610	499			
1	48	349 – 2232	465 – 1122	16/23	0.00012 – 0.0078	0.0023
2	23	735 – 1804	1409 – ∞	12/13	0.001 – 0.016	0.0060
3	15	2409 – 5195	505 – 1530	4/11	0.00013 – 0.00062	0.0004
4	4	1017 – 1902	164 – 320	2/3	0.001 – 0.0031	0.0021
T54	1	70	$\geq$2000	...	...	...

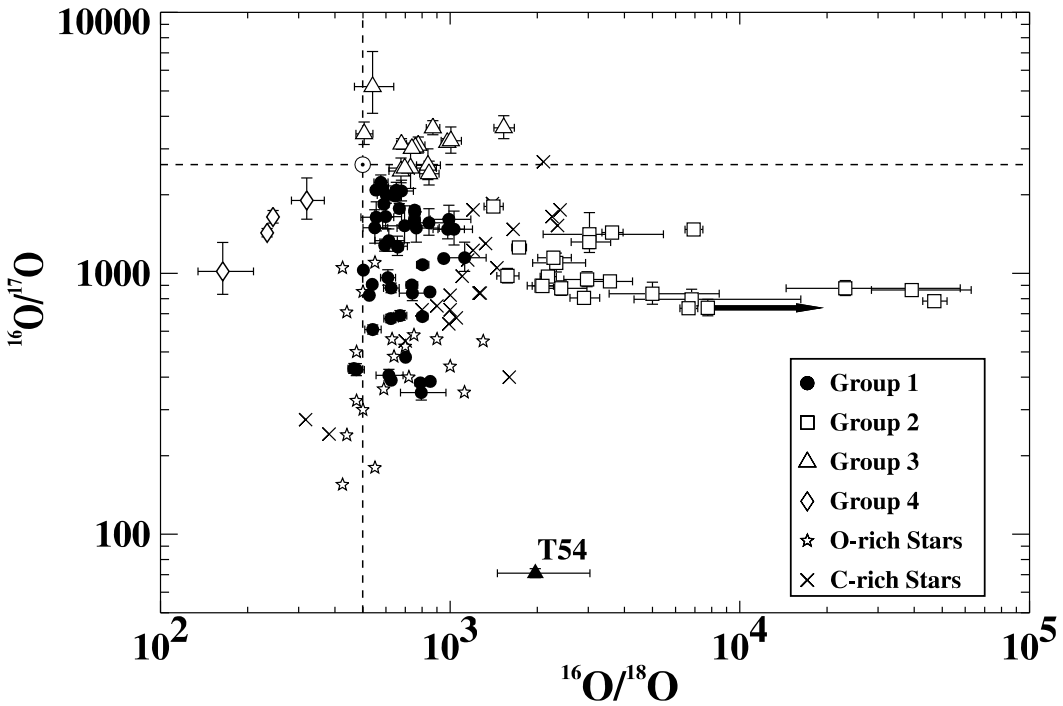

FIGURE 1. O-isotopic ratios of presolar oxide grains (7–16) and red giant stars (17–22). Error bars (typically ∼50%) are not shown for star data points for clarity. Dashed lines indicate solar isotopic ratios in this and subsequent figures.

may well be related to any of these groups. An additional complication is the possibility that ion probe measurements of some of the grains included extraneous O from the sample mounts, diluting the extrasolar signatures. If this was the case, the true compositions of many of the grains may be more extreme (farther away from solar) than indicated on the plot, particularly for grains with depleted ^{17}O and ^{18}O. In any case, the general isotopic trends indicated by the different groups are clear, and most likely reflect different astrophysical processes.

Because of small ($\lesssim 1\mu$m) typical grain sizes and the fact that corundum does not readily incorporate many trace elements in its crystal lattice, there have been few isotopic analyses of elements other than O in presolar oxide grains thus far. Only Mg has been measured in a significant number of grains, but Ti and N have been analyzed in a few cases as well. Fifty-two presolar oxide grains have been analyzed for their Mg-isotopic compositions and Al/Mg ratios. Of these, thirty-five have ^{26}Mg/^{24}Mg ratios much higher than solar, almost certainly due to the *in situ* decay of the short-lived radionuclide ^{26}Al. Inferred initial ^{26}Al/^{27}Al ratios range from 1×10^{-4} up to 1.6×10^{-2}. Table 2 shows the range and mean of ^{26}Al/^{27}Al ratios for the oxide grain groups as well as the fraction of each group that shows evidence for ^{26}Al (see also Fig. 4). The group divisions defined on the basis of O-isotopes are supported by the Mg-Al results, in that both the fraction of grains with ^{26}Mg excesses and the inferred ^{26}Al/^{27}Al ratios increase systematically from

Group 3 to 1 to 2 (there are too few Group 4 grains to make a meaningful comparison). All but two of the grains analyzed for Al-Mg have $^{25}Mg/^{24}Mg$ ratios within analytical errors of the terrestrial value. The exceptions, Orgueil-B (Group 1) and Tieschitz T22 (Group 4), have higher than solar $^{25}Mg/^{24}Mg$ ratios, by 25($\pm$6)% and 13($\pm$3)%, respectively (9,23). The former grain also has unusual Ti isotopic ratios (23), with excesses in all isotopes relative to ^{48}Ti and the terrestrial isotopic ratios. One Group 1 grain has been analyzed for its N isotopic composition; it is depleted in ^{15}N by about 40($\pm$18)%, relative to terrestrial N (11).

III STELLAR SOURCES

The highly unusual isotopic compositions of the oxide grains discussed here clearly establish their presolar, circumstellar origin. Two general questions to be addressed here are: what type or types of stellar environments could have produced the grains, and what new information about these stars can the grains give us? Red giants, supergiants, novae, and supernovae are all believed to be sources of O-rich stardust in the Galaxy (24,25) and spectral features associated with silicates have been observed around all of these except supernovae (26–28). The isotopic compositions of stars, and hence of the dust they produce, reflect both initial compositions and changes that arise as a result of nucleosynthesis and stellar evolution. Our task is to examine what is known about the different evolutionary paths taken by the different stardust sources and infer which ones result in isotopic compositions that are most consistent with the oxide grain data.

The isotopic signatures of most of the grains, depleted ^{18}O, enriched ^{17}O and high $^{26}Al/^{27}Al$ ratios, all point to hydrogen burning (29). Although hydrogen burning occurs in all stars, several lines of evidence point to an origin in low and intermediate mass (1–8 $M_\odot$) red giants and AGB stars for a majority of the grains. First, as shown in Fig. 1, the O-isotopic ratios observed in red giants and AGB stars are similar to those observed in the largest group of oxide grains (Group 1). Second, estimates of dust production in the Galaxy indicate that red giants produce $\sim$90% of the O-rich circumstellar dust (24,25,30). Third, a feature seen in the infrared spectra of many O-rich red giants has been tentatively associated with Al_2O_3 (31,32). Fourth, the isotopic compositions of most of the grains can be quantitatively explained by theoretical models of evolution, nucleosynthesis and mixing in red giants, but not by models of other O-rich dust-producing stars. The fourth point is discussed in detail in the remainder of this section.

A Groups 1 and 3

Presolar oxide grains belonging to Groups 1 and 3 have moderate ^{18}O depletions, relative to solar, and slightly depleted (Group 3) to highly enriched (Group 1) ^{17}O. The similarity of the O-isotopic ratios observed in Group 1 grains to those observed in red giants and AGB stars strongly suggests that these grains formed in such stars

(Fig. 1). Let us thus examine the evolutionary processes that affect the isotopic ratios at the surface of red giants.

For most of a low or intermediate mass star's lifetime, it is powered by H-burning in the core and its surface O-isotopic composition is that of the gas from which the star formed. Following core H-burning, the star leaves the main sequence and becomes a red giant. At this point, deep convection mixes the ashes of main sequence nucleosynthesis into the envelope, a process known as the "first dredge-up" (33). Because partial core H-burning by the CNO-cycles enriches ^{17}O and destroys ^{18}O (29), the surface ^{16}O/^{17}O ratio is decreased and the ^{16}O/^{18}O ratio increased by the first dredge-up (34–36). Following the red giant phase and subsequent core He-burning, the star becomes a thermally pulsing AGB star. Early in the AGB phase, stars of mass M$\gtrsim$3M$_\odot$ undergo a "second dredge-up" which can modify the surface O-isotopic ratios somewhat more (37). The effects of second dredge-up depend on metallicity. For stars of solar metallicity, the second dredge-up does not significantly change the O-isotopic ratios. For lower-metallicity stars, the effect of the first dredge-up is diminished but that of the second dredge-up is enhanced. The net result is that, following both the first and second dredge-ups, stars of a given mass M$\gtrsim$3M$_\odot$ have similar ^{16}O/^{17}O ratios, regardless of their metallicity. Most stars have masses lower than 3M$_\odot$, so the effects of first dredge-up are emphasized in the rest of this paper. However, it should be understood that if any grains formed in more massive stars, their O-isotopic ratios have probably been affected by the second dredge-up as well.

Figure 2 shows model predictions of the effects of first and second dredge-up on O-isotopic ratios for stars of mass M=0.85–9M$_\odot$ and two different metallicities: Z=0.012 and 0.02 (0.6 and 1.0 Z$_\odot$) (37). The initial ^{16}O/^{18}O and ^{16}O/^{17}O ratios of the Z=0.02 stars were assumed to be solar, whereas those of the Z=0.012 stars were adjusted according to a Galactic chemical evolution model (38, see § IV). For low mass (M$\lesssim$2.5 M$_\odot$) stars, the predicted surface ^{16}O/^{17}O ratio following first dredge-up is a steep function of stellar mass; this reflects the increasing depth of dredge-up with increasing stellar mass. For higher mass stars, the ^{16}O/^{17}O ratio is controlled by the destruction of ^{17}O in the nuclear reactions ^{17}O$(p,\alpha)^{14}$N and ^{17}O$(p,\gamma)^{18}$F, which operate more efficiently at the higher temperatures reached in these stars. Except for stars of very low mass (M$\lesssim$1.4M$_\odot$), the final ^{16}O/^{17}O ratio is essentially independent of its initial value since much more ^{17}O is mixed to the surface than was initially present. Substantial variations exist between different published predictions of ^{16}O/^{17}O as a function of stellar mass in red giants (39). For low-mass stars, these differences reflect mainly the different treatments of convection; for higher-mass stars, they are a result of large uncertainties in the cross sections for the ^{17}O destruction reactions. Dredge-up calculations carried out using a recent, highly accurate determination of these reaction rates (40,41) agree within about 20% with the models shown in Fig. 2.

In contrast to ^{16}O/^{17}O, the predicted ^{16}O/^{18}O ratio following first and second dredge-up is not a strong function of stellar mass. Using the best estimate of the ^{18}O$(p,\alpha)^{15}$N reaction rate, models predict that the first and second dredge-up in-

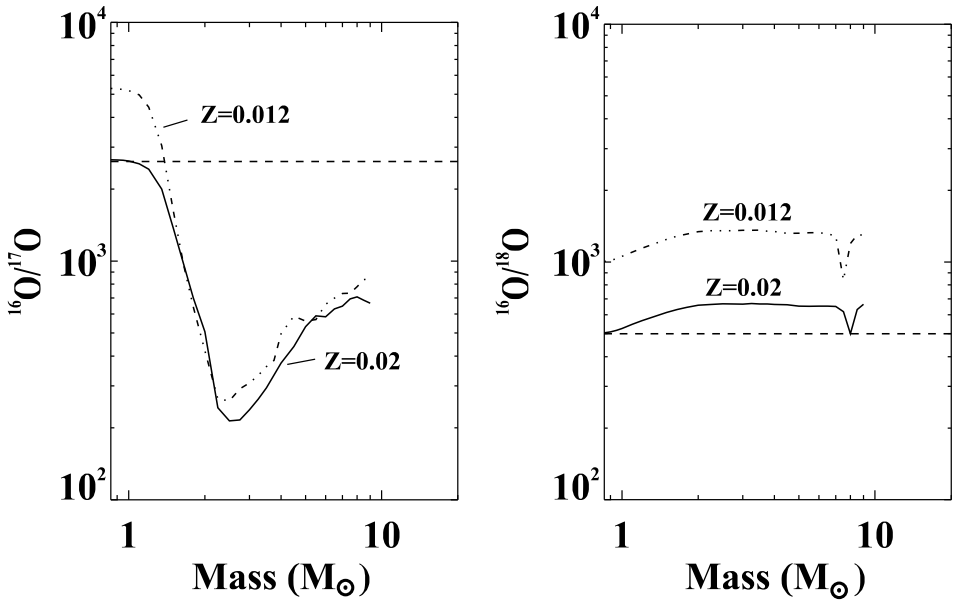

FIGURE 2. Predictions of the O-isotopic ratios in the envelopes of red giant stars following first and second dredge-up, as a function of stellar mass and metallicity. Only stars with mass $\gtrsim 3M_\odot$ undergo second dredge-up (37).

creases the surface $^{16}O/^{18}O$ ratio by 30–50% from its initial value, in stars of mass $M \gtrsim 2M_\odot$ (35–37,39). Stars of lower mass have smaller relative increases (Fig. 2). Larger variations than ∼30–50% between red giants (or grains derived from them) thus require a range of initial compositions (36). The dip in $^{16}O/^{18}O$ observed in Fig. 2 at $\sim 7M_\odot$ has not been confirmed by other models, so it will not be considered here.

The first-dredge-up calculations of Fig. 2 for stars of mass M=0.85–3$M_\odot$ are shown again in Fig. 3, superimposed on the oxide grain data with $^{16}O/^{18}O<1700$. Each open circle represents a different star of a given mass and metallicity. Solid curves connect the predictions for stars of a given metallicity and dotted lines indicate other values extrapolated or interpolated from the calculated values. Group 1 grains clearly have O-isotopic ratios consistent with an origin in red giant stars, provided they formed in several distinct stars with distinct masses and initial compositions. Moreover, the O-isotopic ratios of most Group 3 grains also agree with the predictions, indicating that these grains likely also had an origin in red giants. However, if this is the case, Group 3 grains must have formed in very low-mass stars ($M<1.4M_\odot$) with initial $^{16}O/^{17}O$ and $^{16}O/^{18}O$ ratios higher than the solar values. The most likely explanation for the range of initial O-isotopic compositions required of the progenitor stars of Group 1 and 3 grains is the chemical evolution of the Galaxy; this topic is discussed in more detail below in § IV.

Note that the dredge-up models predict a minimum $^{16}O/^{17}O$ ratio of ∼200-250 for stars of mass $2.5M_\odot$ (Fig. 2). The Group 1 $^{16}O/^{17}O$ distribution, on the other hand, has a lower limit of ∼350, even for a wide range of $^{16}O/^{18}O$ ratios. The

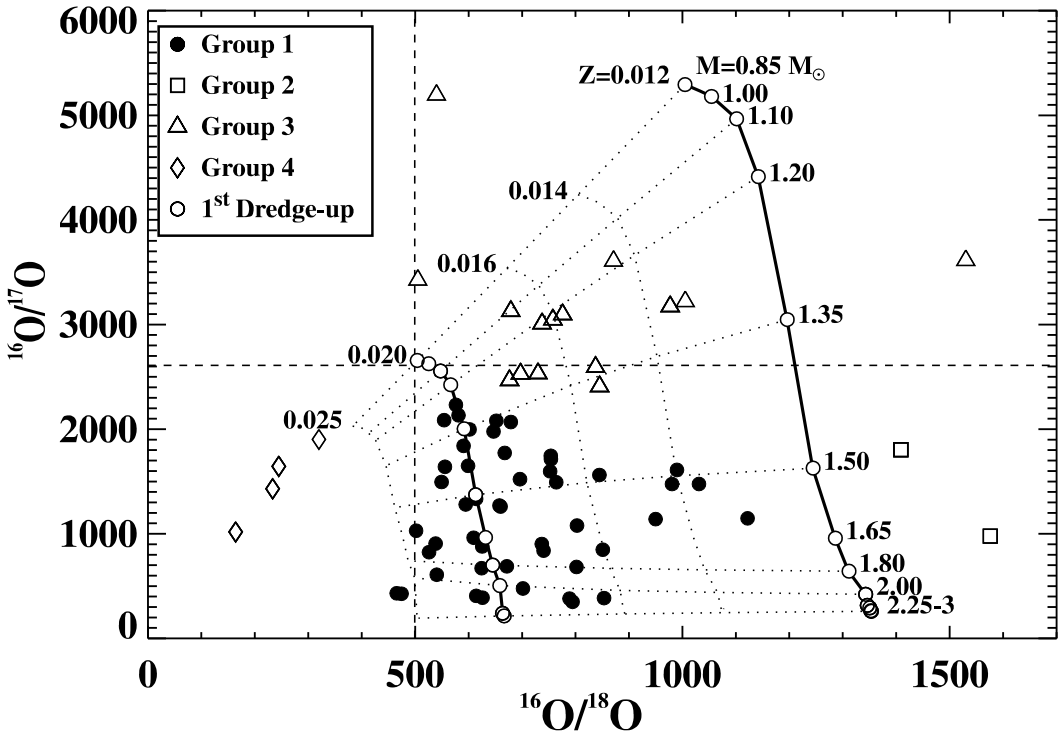

FIGURE 3. Comparison of presolar oxide grain data with predictions of first dredge-up in red giant stars of initial mass 0.85–3$M_\odot$ and metallicity $Z = 0.012$–0.025 (37, Fig. 2). Error bars on grain measurements are not shown for clarity. Each open circle corresponds to predictions for a distinct star. The dotted lines indicate interpolated values for masses and metallicities intermediate to those calculated. Oxide grains belonging to Groups 1 and 3 have isotopic compositions consistent with these predictions, provided that they formed in several different stars with distinct masses and initial compositions.

discrepancy might simply reflect poor statistics and indicate that none of the known Group 1 grains formed in stars of mass M$\sim$2.5–3$M_\odot$. Alternatively, Group 1 grains might have originated in stars with a range of masses including 2.5–3$M_\odot$, and the predicted minima are systematically too low. If this is the case, the presolar oxide grains may provide new constraints on both the depth of dredge-up and on the nucleosynthesis of ^{17}O during core H-burning. The identification of additional Group 1 grains would help to decide the question.

Stars in the AGB phase of their evolution consist of an inert C-O core surrounded by thin He- and H-burning shells and a large convective envelope. They undergo periodic He-shell flashes (thermal pulses) followed by "third dredge-up" episodes, where convection mixes material from the H and He shells with the envelope. The dredged-up material is mostly ^{4}He and ^{12}C and the third dredge-up gradually increases the surface C/O ratio, eventually turning the star into a carbon star. The third dredge-up is unlikely to significantly change the surface O-isotopic ratios from their first and second dredge-up values, since the total amount of the three O isotopes mixed into the envelope is relatively small (36). This is supported by

observations of O-rich AGB stars (21), but a possible rare exception in the case of ^{18}O is discussed below in § III C.

Even though the third dredge-up does not modify the O-isotopic ratios, it is expected to bring ^{26}Al from the H-shell to the surface of AGB stars, and is thus of key importance to the understanding of the presolar oxide grains. Inferred ^{26}Al/^{27}Al ratios are plotted in Fig. 4 against ^{16}O/^{17}O ratios for the ^{26}Mg-enriched oxide grains. Also shown as vertical lines to the right of the plot are the ranges of ^{26}Al/^{27}Al ratios predicted by third dredge-up models (42,43). The predicted ratios are in excellent agreement with the ratios inferred for the grains. However, ∼40% of the Group 1 and 3 grains analyzed for Mg and Al apparently had no ^{26}Al when they formed (Table 2). Since the O-isotopic ratios of these grains reflect the first dredge-up, they must have formed either in red giants before the AGB phase or early in the AGB phase, before many episodes of third dredge-up had occurred. Thus, the presence or lack of ^{26}Al in presolar oxide grains gives information on the timing of mass-loss and grain formation in AGB stars. For example, note that most Group 3 grains did not have ^{26}Al when they formed and the ones with ^{26}Mg excesses have significantly lower inferred ^{26}Al/^{27}Al ratios than Group 1 grains. This suggests that, in

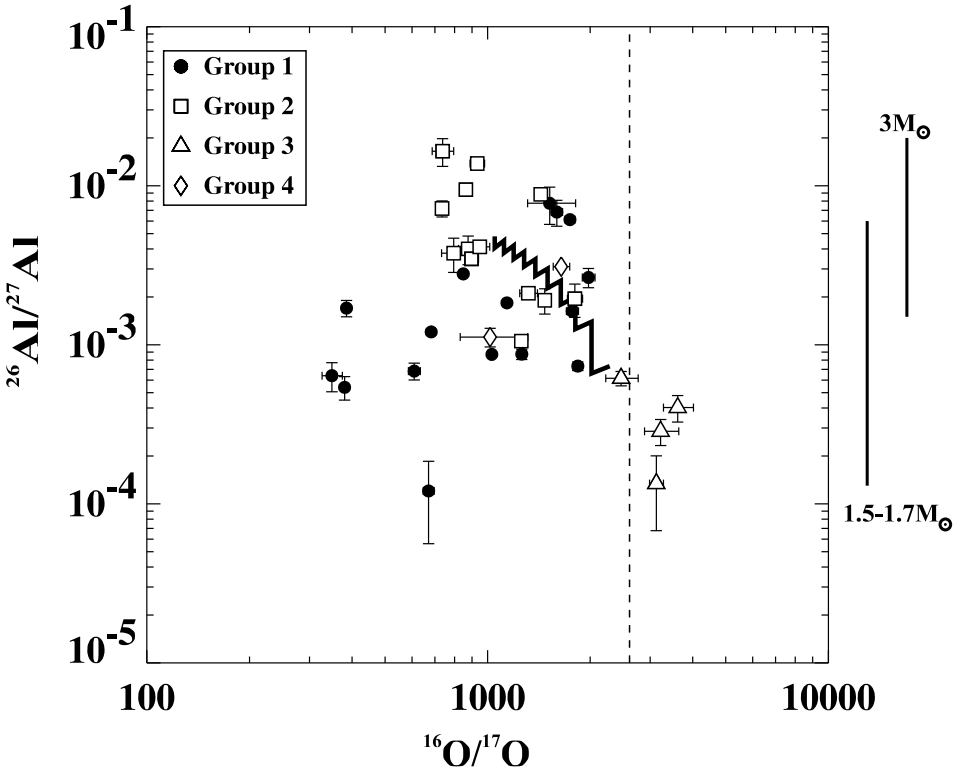

FIGURE 4. Inferred ^{26}Al/^{27}Al ratios plotted against ^{16}O/^{17}O ratios for ^{26}Mg-enriched presolar oxide grains. Vertical lines at right indicate ranges of ^{26}Al/^{27}Al ratios predicted for third dredge-up in AGB stars of mass 3M$_\odot$ (42) and 1.5–1.7M$_\odot$ (43). The jagged line indicates a predicted trend for a 1.2M$_\odot$ star undergoing cool bottom processing during the AGB phases (see the text).

very low-mass ($\lesssim$1.4$M_\odot$) AGB stars, most dust formation occurs prior to the third dredge-up. This is supported by some theoretical models, which show that very low-mass stars lose most of their mass before reaching the AGB (37,44).

Although the AGB phase only occurs in stars of M$\lesssim$8$M_\odot$ (45), more massive stars also dredge up material which has experienced core and shell H-burning into their envelopes. Theoretical models of massive star evolution (41,46,47) suggest that dust grains from red supergiants (of mass 10–25$M_\odot$) have $^{16}O/^{17}O$=600–1100, $^{16}O/^{18}O$=500–1000 and $^{26}Al/^{27}Al$ ratios similar to those predicted for AGB stars (9). Approximately one fourth of the Group 1 oxide grains have these isotopic compositions and thus might have formed in massive red supergiants rather in than low or intermediate mass AGB stars. An origin in the latter seems more likely, since there are far more low-mass stars than high-mass ones, but unknown selection effects (due to grain size, for instance) could bias our sample towards massive stars.

B Group 2

Group 2 grains have ^{17}O enrichments, moderate to extreme ^{18}O depletions, and high inferred $^{26}Al/^{27}Al$ ratios. The $^{16}O/^{17}O$ ratios of these grains are consistent with an origin in low-mass (M<2$M_\odot$) AGB stars, but the degree of ^{18}O depletion is greater than can be explained by the dredge-up of ^{18}O-depleted matter into the envelope of near-solar-metallicity stars. In principle, the high $^{16}O/^{18}O$ ratios of the grains could be due to high initial ratios in the progenitor stars. However, if this were the case, one would expect the Group 2 grains to have a large spread in $^{16}O/^{17}O$, similar to that observed in Groups 1 and 3, instead of the rather limited observed range. Moreover, the most ^{18}O-poor grains would require an origin in extremely low-metallicity stars (*i.e.*, Population II), which are not observed in the Galactic disk. It is therefore more likely that the ^{18}O originally present at the surface of the progenitor stars was destroyed by nuclear reactions; let us consider possible mechanisms.

One proposed mechanism for destroying ^{18}O at the surface of AGB stars is "hot-bottom burning" (HBB). In this process, the base of the convective envelope reaches temperatures high enough for CNO-cycle nuclear reactions to occur, and convection mixes the entire envelope through the hot region (48). Although HBB will lead to very high $^{16}O/^{18}O$ ratios and also produce ^{26}Al, it is believed only to occur in relatively high-mass AGB stars, M=4–7$M_\odot$ (49,50). HBB is thus a highly unlikely explanation for the ^{18}O depletions of Group 2 grains, since the $^{16}O/^{17}O$ ratios of the grains indicate that they formed in stars of lower mass. In fact, detailed calculations have shown that the Group 2 grains have O-isotopic compositions which are inaccessible to HBB with any reasonable model parameters (49).

A more plausible explanation for the isotopic compositions of Group 2 grains is that material at the base of the convective envelope is slowly cycled through the hotter regions near the H-burning shell in low-mass stars, a mixing process that has been named "cool bottom processing" (CBP) (51). CBP has also been

invoked to explain low $^{12}C/^{13}C$ ratios in low-mass red giants (37,52) and high Na and Al abundances observed in some globular cluster giants (53,54). Two different parametrized calculations have addressed the effect of CBP on O-isotopic ratios in low-mass red giants (55) and AGB stars (51). Although these models were very different in their treatment of deep mixing, both gave similar results and were able to reproduce the O-isotopic ratios of Group 2 oxide grains. Essentially, it was found that the envelope O-isotopic composition resulting from CBP depends critically on the maximum temperature seen by the mixed material, but not on the precise details of the mixing mechanism itself. The good agreement between the model predictions and the observations supports a CBP origin for the ^{18}O depletions in Group 2 grains, but this must be confirmed by full stellar evolutionary models including a reasonable physical prescription for deep mixing.

Group 2 grains have, on average, higher $^{26}Al/^{27}Al$ ratios than Group 1 grains, and there is a hint of a negative correlation between $^{26}Al/^{27}Al$ and $^{16}O/^{17}O$ for these grains as well (Fig. 4). These facts suggest that the cool bottom processing that destroyed the ^{18}O in the Group 2 parent stars occurred during the AGB phase, a result previously found by CBP models (37,51). Cool bottom processing is expected to occur along with third dredge-up throughout the AGB phase (although this has not been shown by any self-consistent model), so a correlation between ^{17}O and ^{26}Al enrichment might be expected. To make this statement a little more quantitative, the results of a simple model of the dredge-up of ^{26}Al in a $1.2M_{\odot}$, solar metallicity AGB star undergoing cool bottom processing are presented in Fig. 4. The star was assumed to undergo ten thermal pulses in 1 Myr, during which time CBP continuously decreases the $^{16}O/^{17}O$ ratio from its first dredge-up value of $\sim$2400 to a value of 1600 (51). Following Gallino *et al.* (43), we assumed that each dredge-up episode mixes $\sim 10^{-8}M_{\odot}$ of ^{26}Al into the envelope, which has an assumed mass at the first thermal pulse of $0.24M_{\odot}$ (44). Mass-loss was not taken into account, but the ^{26}Al in the envelope was allowed to decay during the 10^5y between thermal pulses. The resulting predicted isotopic trend is shown as the black jagged line in Fig. 4. This line agrees roughly with the general Group 2 trend, but it does not reach $^{26}Al/^{27}Al$ ratios as high as those observed in many grains. In fact, if the star is assumed to evolve further so that its $^{16}O/^{17}O$ ratio decreases to the lowest observed Group 2 value, the predicted $^{26}Al/^{27}Al$ ratio levels out at a value of $\sim$0.007, a factor of 2 lower than the highest observed value. There are two ways in which higher $^{26}Al/^{27}Al$ ratios might be obtained. First, the predicted ratio depends strongly on the mass of the envelope into which the dredged-up ^{26}Al is mixed. If our model star has an assumed fixed mass-loss rate of $2\times10^{-7}M_{\odot}$/y, it loses most of its envelope at the end of 1 My, and we obtain a $^{26}Al/^{27}Al$ ratio of 0.01. Second, the O-isotopic ratios of Group 2 grains are best-explained by CBP at a maximum temperature of $\sim 33\times10^6$K (51) and synthesis of ^{26}Al is marginally possible at this temperature (42). Thus, cool bottom processing might produce ^{26}Al directly, resulting in $^{26}Al/^{27}Al$ ratios in the envelope that are higher than those obtained solely by third dredge-up. No models have yet addressed the production of ^{26}Al by cool bottom processing in AGB stars. A potentially diagnostic indicator is the $^{25}Mg/^{24}Mg$ ratio

of extreme Group 2 presolar oxide grains; ^{26}Al production comes at the expense of ^{25}Mg, so this ratio should be lower if high ^{26}Al/^{27}Al ratios are due to CBP rather than third dredge-up. In this regard, it would be useful to find presolar spinel grains with Group 2 O-isotopic signatures. The above discussion underscores the need for improved modeling of low-mass AGB stars, in order to better understand the interactions between CBP, third dredge-up, mass-loss and grain formation.

Recent models raise the alternative possibility that some Group 2 grains formed in Wolf-Rayet stars, very massive ($M>25M_{\odot}$) stars whose outer layers are shed by extreme mass-loss (56). As these stars evolve from the main sequence to the O- and N-rich WN phase, their surface O-isotopic and ^{26}Al/^{27}Al ratios are predicted to evolve in a similar fashion to those of AGB stars undergoing cool bottom processing, and they are thus possible sources of Group 2 oxide grains. However, mass-loss rates are much higher during the WN phase than during the stages leading up to it, and WN stars are predicted to have ^{16}O/^{18}O ratios of 10^5–10^6 (56). One might thus expect most Wolf-Rayet oxide grains to have larger ^{18}O depletions than observed in most of the grains. In fact, dust formation has only been observed in later-type C-rich Wolf-Rayet stars (57) and not in O-rich Wolf-Rayet stars. This observation and the fact that Wolf-Rayet stars are much rarer in the Galaxy than stars of lower mass suggest that AGB stars are a more likely source of Group 2 grains than Wolf-Rayet stars, but clearly much more work needs to be done.

C Group 4

Group 4 grains have ^{18}O excesses, relative to solar, and ^{16}O/^{17}O and ^{26}Al/^{27}Al ratios similar to those of Group 2 grains. One grain, T22, also has excesses of ^{25}Mg and ^{26}Mg. The ^{16}O/^{17}O and inferred ^{26}Al/^{27}Al ratios of these grains are consistent with an origin in low-mass AGB stars, but the origin of the excess ^{18}O in such stars is unknown. One possibility is that ^{18}O is produced in the He-shell by α captures on ^{14}N during early thermal pulses, and is dredged-up to the surface before it can be converted to ^{22}Ne (44,58). So far, no model has self-consistently predicted dredge-up of ^{18}O in AGB stars. Moreover, the O-isotopic compositions observed in AGB stars (21, Fig. 1) and Group 1 oxide grains indicate that most AGB stars do not dredge-up large amounts of ^{18}O. The existence of Group 4 grains suggests that such dredge-up might occur in special cases, however, and indicates the need for detailed modeling to see if this is a viable scenario. Alternatively, the ^{18}O excesses observed in Group 4 grains might reflect a high initial ^{18}O abundance in the parent stars. Extrapolating from the dredge-up calculations shown in Figs. 2 and 3, this would require that the grains formed in stars with metallicities from 1.6–3$Z_{\odot}$ and low masses ($M\sim1M_{\odot}$). It is highly unlikely that stars of such low mass and high metallicity were present to contribute dust to the presolar cloud, making this scenario less attractive than third dredge-up as an explanation for the low ^{16}O/^{18}O ratios of Group 4 grains. Note that the ^{25}Mg excess observed in T22 is not very diagnostic, since such an excess is expected both from n-capture reactions

in AGB stars (59) and in the initial compositions of high-metallicity stars (60).

D T54

Grain T54 has $^{16}O/^{17}O$=71, much lower than any of the other grains, and a substantial ^{18}O depletion ($^{16}O/^{18}O \geq 2000$). No known stellar source is predicted or observed to have this O-isotopic composition. However, one can imagine complicated scenarios where mass-transfer from a binary companion might play a role. For example, T54 might have formed in a star which had accreted matter highly-enriched in ^{17}O from a hot-bottom burning AGB star companion and then undergone its own first dredge-up. However, such a picture is *ad hoc* and would certainly need to be confirmed by models.

On the other hand, T54 was completely destroyed during the ion microprobe analysis and the few ^{18}O atoms measured in this grain could simply be due to a blank contribution from the sample mount or a tiny neighboring Solar System grain. If so, the true $^{16}O/^{18}O$ ratio of this grain is similar to ∞. This composition is close to that predicted for extreme hot-bottom burning in a $7M_{\odot}$ AGB star (49), although the observed $^{16}O/^{17}O$ ratio is slightly lower than the predicted final ratio of $\sim$110.

E Summary of Stellar Sources

The O-isotopic ratios of the presolar oxide grains are shown again in Fig 5, together with the trends discussed above for red giants and AGB stars (dredge-up, cool bottom processing and hot-bottom burning) and Wolf-Rayet stars in the WN phase. Also shown is the expected evolution of O-isotopic ratios in the Galaxy (38, see next section) and the predicted compositions of novae (61,62) and different interior zones of a $25M_{\odot}$ Type II supernova (63). Clearly, the grains of Groups 1–4 are best explained by an origin in red giants and AGB stars, although the Group 4 grains require atypical dredge-up of ^{18}O to occur in some AGB stars. The source of grain T54 is unclear, but might have been an AGB star undergoing hot-bottom-burning. None of the grains discussed here have compositions consistent with an origin in novae or supernovae. In principle, grains could condense in the O-rich envelope of a Type II supernova, with O-isotopic compositions in the lower part of the Group 1 field. However, only $\sim$10% of the ejected O is from the envelope (63), so most supernova oxides should form from the inner ^{16}O-rich zones. Moreover, observations indicate that dust formation in Supernova 1987A occurs mainly in the inner zones (64). It is therefore highly unlikely that any of the Group 1 grains formed in supernovae (although some could have condensed around red supergiants prior to a supernova explosion).

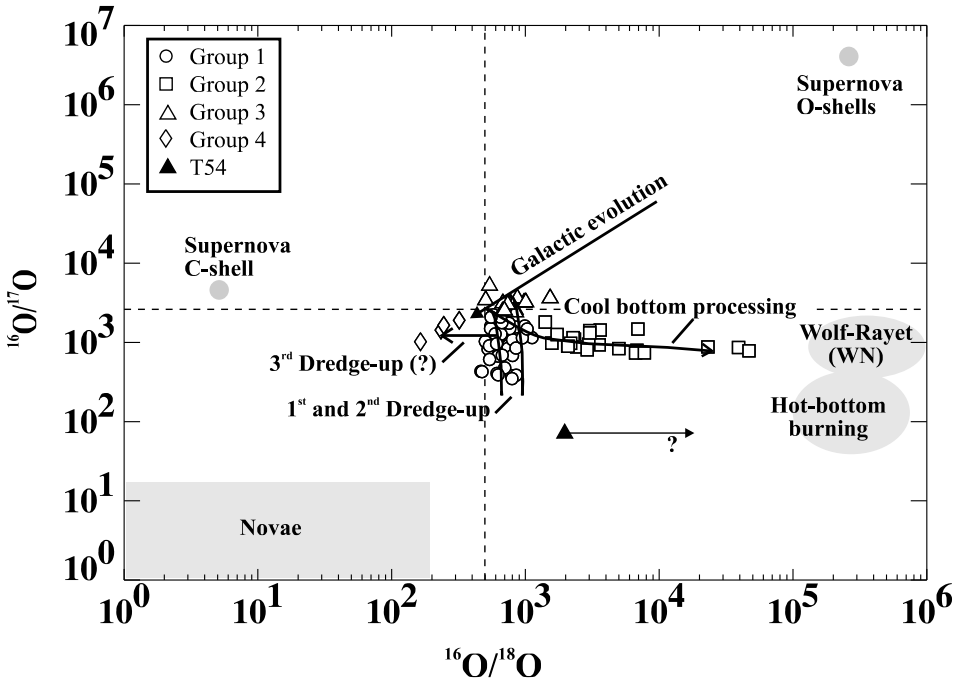

FIGURE 5. O-isotopic ratios of presolar oxide grains and predictions for different astrophysical sites and processes: Galactic chemical evolution (38), dredge-up in red giants, red supergiants and/or AGB stars (37,58), cool bottom processing in low-mass AGB stars (51,55), hot-bottom burning in intermediate-mass AGB stars (49), Wolf-Rayet stars (56), novae (61,62) and O-rich and C-rich shells of a $25M_{\odot}$ Type II supernova (63).

IV GALACTIC CHEMICAL EVOLUTION AND THE AGE OF THE GALAXY

Thus far emphasis has been mainly on the nucleosynthetic and stellar evolutionary processes that are recorded in the isotopic signatures of presolar oxide grains. In this section, it is shown how the grains also give information on Galactic evolution. As previously discussed, the isotopic compositions of Group 1 and 3 oxide grains are consistent with red giant and AGB star models only if they formed in a range of stars with distinct masses and initial O-isotopic compositions. Variations in the chemical compositions of new stars are thought to arise naturally as a consequence of the chemical (abundance) evolution of the Galaxy. Addressed here is the question of whether the inferred distribution of O-isotopic ratios in the parent stars of the Group 1 and 3 grains is consistent with what is known about the evolutionary history of the Milky Way. Furthermore, a new method for constraining the age of the Galaxy using the presolar oxide grain data is briefly discussed.

As the Galaxy evolves, freshly synthesized elements from dying stars are returned to the interstellar medium where they are incorporated into new stars. As a result, the abundance of the heavy elements (*i.e.*, metallicity) increases throughout the history of the Galaxy, and stars formed at different times (and Galactocentric ra-

dius) have, on average, different chemical and isotopic compositions. Because the different isotopes of O are synthesized by different processes, their relative abundances in the interstellar medium, and hence in new stars, are expected to change as the Galaxy evolves. The isotope ^{16}O is considered a "primary" nucleosynthetic product, since it can be produced in a star of initially pure H and He (Z=0). The synthesis of ^{17}O and ^{18}O, on the other hand, requires pre-existing CNO nuclei, so these O isotopes are "secondary" nuclei. To a good approximation, secondary/primary ratios are expected to increase linearly with metallicity (60). Also, since the average metallicity of the Galaxy increases over time (65), initial ^{17}O/^{16}O and ^{18}O/^{16}O ratios should be lower in older stars than in younger ones. This basic picture of O-isotopic evolution (normalized to the solar O-isotopic ratios) is indicated on Fig. 5 by the arrow labeled "Galactic evolution." A linear relationship between O-isotopic ratios and metallicity has been found by detailed Galactic chemical evolution models as well (38,66), and was used to relate the initial compositions of red giants to their metallicity in the dredge-up models discussed in this paper.

The first-dredge-up predictions shown in Figs. 2 and 3 define an irregular grid in O-isotopic space, from which we can infer the masses and metallicities of oxide grain parent stars. The inferred mass and metallicity distributions of the parents of Group 1 and 3 grains are shown in Fig. 6. The two Group 3 grains with solar ^{16}O/^{18}O ratios are not included, since their compositions are not consistent with the dredge-up models and they thus might have a different origin than the rest of the grains. There are a number of factors which complicate the interpretation of these distributions. First, it has been assumed that all of the parent stars had masses less

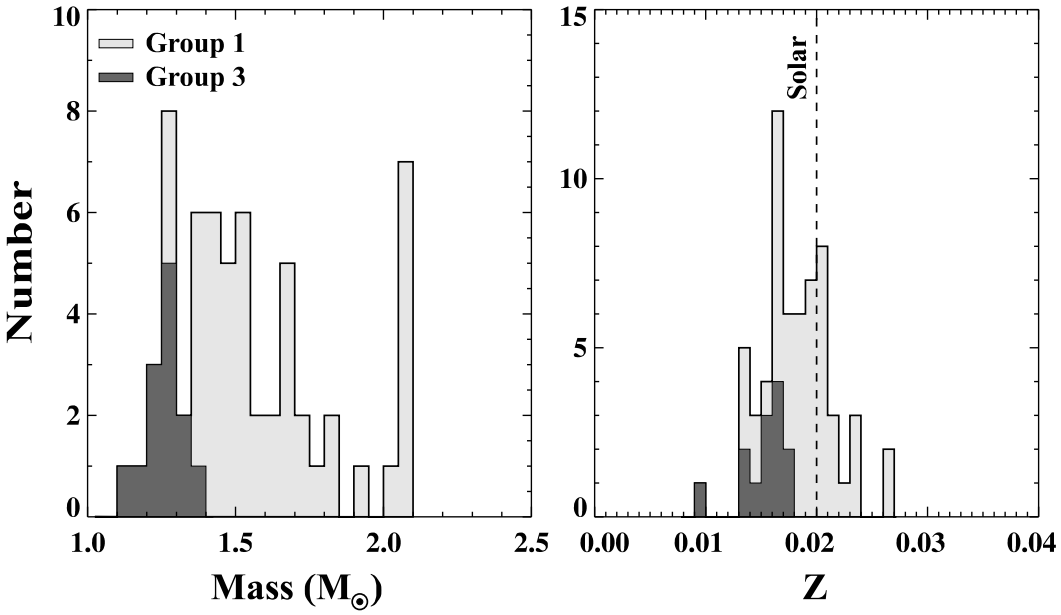

FIGURE 6. Masses and metallicities of the red giant progenitors of Groups 1 and 3 presolar oxide grains, inferred from the first-dredge-up models of Figs. 2 and 3.

than 2.5$M_\odot$, but in fact grains with $^{16}O/^{17}O \lesssim 1000$ could have come from more massive stars (Fig. 2). The peak at $M \approx 2M_\odot$ in Fig. 6 might suggest that some of the grains do indeed come from stars of higher mass, if the total production of micron-sized stardust is a decreasing function of stellar mass. Second, grains from high-metallicity (Z=0.02–0.03) stars are under-represented here, since they have $^{16}O/^{18}O$ ratios in the region missed by ion imaging searches for presolar oxides (see also ref. (30)). These two difficulties have little effect on the remainder of the discussion since we are more interested in the grains from low-mass, low-metallicity stars. A potentially more damaging problem is the dependence of the metallicity distribution on the assumed relationship between initial O-isotopic ratios and metallicity used in the dredge-up models; if the assumed trend is incorrect, the inferred Z values (and for $M \lesssim 1.5M_\odot$, the inferred masses) may be systematically off. This is discussed further below.

It is clear from Fig 6 that the progenitor stars of Group 3 presolar oxide grains not only had lower masses than those of Group 1 grains, as discussed in § III A, but also had, on average, lower metallicities. This is easily understood in terms of Galactic chemical evolution. In order for the presolar oxide grains to have been present at the time of Solar System formation, their parent stars must all have ended their lives close to this time, probably within $\sim 10^8$ years. Since low-mass stars evolve more slowly than higher-mass stars, this means that the Group 3 parents formed earlier than the Group 1 parents and consequently had lower metallicity. To explore this relationship between mass and metallicity in more depth, the progenitor stars are plotted on an "age-metallicity" diagram (Fig. 7), and compared with astronomical observations and theoretical predictions. In this plot, the inferred metallicity for each grain, divided by the solar value, is plotted against the minimum time before today when the parent star formed. The latter was obtained by adding the age of the Solar System, 4.6 Gyr, to the lifetime predicted for a star of the given mass and metallicity (67). Also shown, as open squares, are the observed metallicities (Fe/H) and inferred ages of disk dwarf stars of the same Galactocentric radius as the Sun (65). The y-error bars for these points indicate the observed spread in metallicity for stars within different age bins, indicated by the horizontal bars. The thick black curve is the age-metallicity relation predicted by the detailed model of Galactic chemical evolution of Timmes *et al.* (38); the dot-dot-dashed curves above and below the black curve represent the theoretical trend scaled up and down respectively, by 35%

There is surprisingly good agreement between the inferred distribution of grain parent stars and the theoretical age-metallicity relation; in particular, the predicted age-metallicity relation passes close to the center of the progenitor star field. Also, the shape of the distribution is consistent with there having been a $\sim \pm 35\%$ range around the average metallicity for parent stars formed at different times in the Galaxy (dot-dot-dashed curves). The overall consistency of the Group 1 and 3 grain data with models of Galactic chemical evolution, first dredge-up, and stellar lifetimes strongly supports the conclusion that the grains formed in red giants and that chemical evolution significantly influenced the grains' compositions. How-

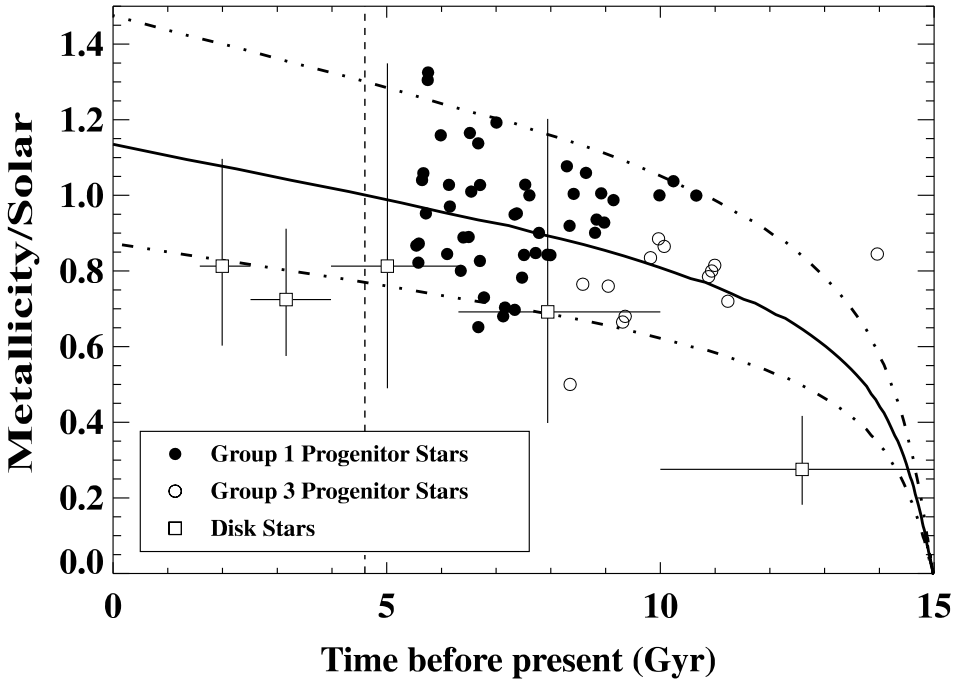

FIGURE 7. Metallicity of oxide grain progenitor stars plotted against the time at which the star must have formed in order to contribute dust to the early Solar System. White squares indicate the binned observational data of Edvardssen *et al.* (65) of disk dwarf stars at the solar Galactocentric radius. The solid curve is a theoretical age-metallicity relation of Timmes *et al.* (38); the dot-dot-dashed curves are the same relation arbitrarily scaled up or down by a factor of 1.35. The total metallicity (Z) is plotted for the grain progenitors and the theoretical curves; Fe/H is plotted for stellar observations. Although the iron abundance and total metallicity are not directly comparable, the differences between the two are probably smaller than the ranges of values on the plot.

ever, although the progenitor stars overlap with the observed disk stars, the average metallicity of the grain parent stars formed at any given time (and that predicted by the model) is higher than the average observed in current stars that formed at the same time. Another discrepancy suggested by Fig. 7 is that the apparent metallicity spread of $\pm$35% implied by the grain data is smaller than that observed in disk stars, but it is not clear whether or not this difference is significant, given the uncertainties in both the models and observations.

Given that some of the presolar oxide grains originated in low-mass, low-metallicity red giants, their compositions may be used to constrain the age of our Galaxy (16). Since stars produce dust at the end of their lives, in order for a star to have provided dust to the Solar System, the age of the Galaxy must be larger than the lifetime of the star added to that of the Sun, *i.e.*, the values plotted for grain progenitors on the abscissa of Fig. 7. These values are thus lower limits on the Galactic age. If the one star plotting at $\sim$14 Gyr that is not within the main distribution is excluded, the data indicate that the Milky Way disk is at least 10–11 Gyr old. The excellent agreement of the Galactic chemical evolution model with

the grain data suggests that the age of the Galaxy is close to that assumed by the model, 15 Gyr; a detailed analysis of the data gives an estimate of 14.4 Gyr (16). The systematic uncertainties affecting this estimate, due primarily to uncertainties in chemical evolution and stellar dredge-up models, are potentially large (several Gyr) and discussed in detail in (16).

The inferred mass and metallicity values of the progenitors of presolar oxide grains depend on the assumption that the $^{17}O/^{16}O$ and $^{18}O/^{16}O$ ratios increase in a linear fashion with metallicity and that they have the solar values in stars of solar metallicity. This Galactic chemical evolution trend for O-isotopes is by no means certain, however. Some information on the chemical evolution of isotopic ratios is obtained from radio observations of molecular clouds throughout the Galaxy. Such observations have found a remarkably uniform $^{18}O/^{17}O$ ratio of 3.6 and positive gradients of $^{16}O/^{17}O$ and $^{16}O/^{18}O$ with Galactocentric radius (68,69,66). These data support the ideas that ^{17}O and ^{18}O are both secondary isotopes and have increased uniformly with metallicity, relative to primary ^{16}O. However, there are important discrepancies between the elemental and isotopic abundances observed in molecular clouds and those of the Solar System, so the normalization of the assumed O-isotopic evolution trend to solar values may be invalid. In particular, the Sun seems to have a higher relative abundance of ^{18}O than expected for stars of its age and Galactocentric radius. Proposed explanations for the "atypical" composition of the Sun include that the protosolar cloud from which the Sun formed was preferentially enriched in material from massive stars (70,66), and that the Sun formed at a smaller Galactocentric radius than that of its current position (71,72) and later migrated out to its current orbit. In any case, the good agreement between the various models discussed above and the compositions of the presolar oxide grains suggests that the assumed evolution of O-isotopic ratios is not too far removed from reality, at least for the material that went into the making of the Solar System. That is, the grains might reflect a "local" Galactic chemical evolution that resulted in the composition of the Sun, but which differed in detail from the average chemical history of the Galaxy as a whole. The isotopic analysis of additional elements in presolar oxide grains would help shed light on the issues discussed here by providing additional constraints on the influence of Galactic chemical evolution on the grain compositions. For example, Huss *et al.* (73) have argued that chemical evolution might provide a natural explanation for the unusual Mg and Ti-isotopic ratios observed in one presolar Al_2O_3 grain, Orgueil-B. Similarly, Galactic chemical evolution has been invoked to explain the Si and Ti isotopic compositions of presolar SiC in meteorites (43,74–76).

V OXIDE GRAIN PUZZLES

It is clear from the preceding discussions that the origins of most presolar oxide grains, in particular those belonging to Groups 1 and 3, are reasonably well understood in terms of both the evolution of the Galaxy and stellar evolutionary processes

in red giants and AGB stars. However, there are still a number of mysteries concerning presolar oxide grains. The most pressing questions yet to be answered about the isotopic data are: 1) what were the sources of the Group 4 grains and grain T54? and 2) what is the physical cause of the extra mixing (cool bottom processing) that probably occurred in the parent stars of Group 2 grains? Both of these issues are likely to be resolved with improved stellar modeling and with the identification of more grains.

Perhaps the most important unanswered question concerning presolar oxides is related to their abundance. The meteoritic concentration of presolar oxide grains of size $\gtrsim 0.5\mu$m is much lower than that of presolar SiC in the same size range ($\sim$10 ppb versus $\sim$5 ppm). This is in sharp contrast to expectations based on what is known about dust production in the Galaxy. With the assumptions that all Al in O-rich red giants condenses into Al_2O_3 and all Si in C-stars into SiC, and by taking into account astronomical estimates of the relative dust production rates of C-rich and O-rich red giants in the Galaxy, the mass ratio of presolar SiC to presolar Al_2O_3 in meteorites is predicted to be 1–10 (9,30), much lower than the ratio observed in different meteorites. Al_2O_3 should not be preferentially destroyed, relative to SiC, either by processes in space or by the chemical treatments used to isolate presolar grains from meteorites (7). In fact, SiC should be more readily destroyed than Al_2O_3 in the oxidizing conditions of the interstellar medium and early Solar System.

The low abundance of presolar oxides might be explained if presolar Al_2O_3 has a finer grain size distribution than presolar SiC. The size of grains condensing in a stellar atmosphere depends to a large extent on mass-loss rates (77), which are predicted to be higher in the latest C-rich stages of AGB star evolution than in the earlier O-rich stages (78). A grain size distribution that is finer for Al_2O_3 stardust than for SiC stardust is thus plausible on theoretical grounds. However, the size distribution of dust observed around O-rich red giants and AGB stars is similar to that observed around C-rich AGB stars (79) and micron-sized grains are observed around both C-rich and O-rich red giants (79,80). Alternatively, the underabundance of presolar oxide grains might indicate that only a small fraction of the Al in AGB winds condenses into Al_2O_3. Most circumstellar and interstellar O-rich dust is in the form of silicates, not refractory oxides such as Al_2O_3 and $MgAl_2O_4$, so a major fraction of Al in AGB atmospheres might condense into silicates. This is supported by the results of Begemann *et al.* (32) who found that at most 25% of the available Al can be in the form of Al_2O_3 in those O-rich AGB stars with spectroscopic evidence for the presence of crystalline Al_2O_3. Presolar silicate grains, if present in meteorites, would have been destroyed by the chemical treatments of the meteorites studied thus far.

Another major puzzle is the fact that no oxide grains have been identified that appear to have condensed in Type II supernova ejecta. Grains of SiC, graphite, and Si_3N_4 grains with isotopic compositions indicating a supernova origin have all been found in meteorites (81–83). O-rich dust grains should form in supernovae in addition to the reduced phases, since much more O than C is ejected in super-

nova explosions (63,47). Estimates based on published calculations of supernova yields (47) suggest that Al_2O_3 grains from supernovae should make up 10–70% of presolar oxide grains in meteorites (9,30). No evidence for extremely ^{16}O-enriched refractory oxide grains larger than $\sim 0.1 \mu$m in meteorites has yet been found (4,9) and supernova-produced Al_2O_3 is thus markedly underabundant in the current data set. As in the case of the overall paucity of presolar oxide grains in meteorites, the lack of supernova grains might indicate that most Al does not condense into Al_2O_3 or that supernovae underproduce oxide grains larger than $\sim 0.1 \mu$m, relative to AGB stars. The latter possibility is supported by the calculations of Kozasa *et al.* (84) for dust in supernova 1987A. The lack of ^{16}O-rich supernova oxides is important from the point of view of meteoritics as well, since the presence of such grains has been proposed for over twenty years to explain ^{16}O enrichments in refractory inclusions in meteorites (85–87). That presolar grains highly enriched in ^{16}O have not been found might indicate the need to look elsewhere for an explanation for the meteoritic ^{16}O excesses, for example to non-mass-dependent fractionation processes (88).

VI SUMMARY

Ninety-two meteoritic oxide grains (mostly Al_2O_3) have been identified as presolar grains on the basis of their highly unusual isotopic compositions. The grains have been divided into four groups on the basis of their O-isotopic ratios; one grain, T54, is ungrouped. *Group 1 and 3* grains most likely formed in low- or intermediate-mass red giants and asymptotic giant branch (AGB) stars. Their O-isotopic ratios are well explained by models of Galactic chemical evolution and the first dredge-up. The inferred prior presence of ^{26}Al in many of the grains can be quantitatively explained by third dredge-up in AGB stars. The grains without evidence for ^{26}Al must have formed before the thermally pulsing AGB phase. The compositions of Group 3 grains indicate that the Galaxy is 14–15 billion years old, but this estimate has potentital systematic errors of several Gyr. Large ^{18}O depletions in *Group 2* grains indicate that they probably formed in low-mass AGB stars undergoing cool bottom processing. The high inferred initial ^{26}Al/^{27}Al ratios of Group 2 grains suggest that cool bottom processing can synthesize ^{26}Al in AGB envelopes, a possibility not yet addressed by models. An alternative, but less likely, possible source of Group 2 grains is in Wolf-Rayet stars prior to the WN phase of evolution. *Group 4* grains are enriched in ^{18}O, suggesting that some AGB stars dredge up this isotope in early thermal pulses. Alternatively, these grains might have formed in low-mass AGB stars of unusually high metallicity. *Grain T54* is extremely enriched in ^{17}O and depleted in ^{18}O. Its composition might reflect hot-bottom burning in an intermediate mass AGB star. Presolar oxide grains are underabundant in meteorites, relative to presolar SiC grains, by one to three orders of magnitude. Explanations include the possibility that most Al in AGB stars condenses into silicates and not into Al_2O_3 and that presolar oxide grains in meteorites

have a finer grain size distribution than presolar SiC grains. Although both theoretical models and ^{16}O enrichments in meteorites suggest that a significant fraction of presolar oxide grains should have formed in Type II supernovae, no grains with extreme ^{16}O enrichments indicating such an origin have been found.

Although presolar oxide grains in meteorites are somewhat difficult to identify, they clearly provide important astrophysical information and are thus worth the effort required to locate them. As has happened with the detailed characterization of large numbers of presolar SiC and graphite grains, we should expect many new surprises and insights as more and more presolar oxide grains are identified in meteorites. Improvements in astrophysical models and astronomical observations will no doubt aid in the resolution of some of the outstanding problems associated with the current presolar oxide grain data set as well.

ACKNOWLEDGEMENTS

I would like to thank Conel Alexander, Robert M. Walker and Ernst Zinner for their close involvement in this work. I acknowledge the role of Xia Gao in preparing meteoritic residues and that of Peter Hoppe in the development of ion image mapping. I thank Marcel Arnould, Arnold Boothroyd, Donald Clayton, Ramanath Cowsik, Gary Huss, Frank Timmes, and Stan Woosley for sharing results and for useful scientific discussions.

REFERENCES

1. Lewis, R. S., Tang, M., Wacker, J. F., Anders, E., and Steel, E., *Nature* **326**, 160–162, 1987.
2. Bernatowicz, T., Fraundorf, G., Tang, M., Anders, E., Wopenka, B., Zinner, E., and Fraundorf, P., *Nature* **330**, 728–730, 1987.
3. Amari, S., Anders, E., Virag, A., and Zinner, E., *Nature* **345**, 238–240, 1990.
4. Zinner, E. and Tang, M., *Lunar Planet. Sci.* **19**, 1323–1324, 1988.
5. Huss, G. R., Hutcheon, I. D., Wasserburg, G. J., and Stone, J., *Lunar Planet. Sci.* **23**, 563–564, 1992.
6. MacPherson, G. J., Davis, A. M., and Zinner, E. K., *Meteoritics* **30**, 365–386, 1995.
7. Hutcheon, I. D., Huss, G. R., Fahey, A. J., and Wasserburg, G. J., *ApJ* **425**, L97–L100, 1994.
8. Nittler, L. R., Alexander, C. M. O'D., Gao, X., Walker, R. M., and Zinner, E. K., *Nature* **370**, 443–446, 1994.
9. Nittler, L. R., Alexander, C. M. O'D., Gao, X., Walker, R. M., and Zinner, E., *ApJ*, in press, 1997.
10. Nittler, L. R., Walker, R. M., Zinner, E., Hoppe, P., and Lewis, R. S., *Lunar Planet. Sci.* **24**, 1087–1088, 1993.
11. Strebel, R., Hoppe, P., and Eberhardt, P., *Meteoritics and Plan. Sci.* **31**, A136, 1996.

12. Huss, G. R., Fahey, A. J., Gallino, R., and Wasserburg, G. J., *ApJ* **430**, L81–L84, 1994.
13. Huss, G. R., unpublished data.
14. Nittler, L. R., Alexander, C. M. O'D., Gao, X., Walker, R. M., and Zinner, E. K., "Oxygen-rich stardust in meteorites", In *Nuclei in the Cosmos III*, edited by M. Busso, R. Gallino, and C. M. Raiteri. New York: AIP, 1995, pp. 585–589.
15. Gao, X., Amari, S., Messenger, S. R., Nittler, L. R., Swan, P., and Walker, R. M., *Meteoritics and Plan. Sci.* **31**, A48, 1996.
16. Nittler, L. R. and Cowsik, R., *Phys. Rev. Lett.* **78**, 175–178, 1997.
17. Harris, M. J. and Lambert, D. L., *ApJ* **281**, 739–745, 1984.
18. Harris, M. J. and Lambert, D. L., *ApJ* **285**, 674–682, 1984.
19. Harris, M. J., Lambert, D. L., Hinkle, K. H., Gustafsson, B., and Eriksson, K., *ApJ* **316**, 294–304, 1987.
20. Harris, M. J., Lambert, D. L., and Smith, V. V., *ApJ* **325**, 768–775, 1988.
21. Smith, V. V. and Lambert, D. L., *ApJS* **72**, 387–416, 1990.
22. Kahane, C., Cernicharo, J., Gomez-Gonzalez, J., and Guélin, M., *A&A* **256**, 235–250, 1992.
23. Huss, G. R., Fahey, A. J., and Wasserburg, G. J., *Meteoritics* **29**, 475–476, 1994.
24. Gehrz, R. D., *ARA&A* **26**, 377–412, 1988.
25. Whittet, D. C. B., *Dust in the Galactic Environment*, New York: Institute of Physics, 1992.
26. Treffers, R. and Cohen, M., *ApJ* **188**, 545–552, 1974.
27. Little-Marenin, I. R., *ApJ* **307**, L15–L19, 1986.
28. Bode, M. F., Evans, A., Whittet, D. C. B., Aitken, D. K., Roche, P. F., and Whitmore, B., *Mon. Not. R. Astron. Soc.* **207**, 897, 1984.
29. Clayton, D. D., *Principles of Stellar Evolution and Nucleosynthesis*, New York: McGraw-Hill, 1983.
30. Alexander, C. M. O'D., this volume.
31. Onaka, T., De Jong, T., and Willems, F. J., *A&A* **218**, 169–179, 1989.
32. Begemann, B., Dorschner, J., Henning, T., Mutschke, H., Guertler, J., Koempe, C., and Nass, R., *ApJ* **476**, 199–208, 1997.
33. Iben, Jr., I., *ARA&A* **5**, 571–626, 1967.
34. Landré, V., Prantzos, N., Auger, P., Bogaert, G., Lefebvre, A., and Thibaud, J. P., *A&A* **240**, 85–92, 1990.
35. Dearborn, D. S. P., *Phys. Rep.* **210**, 367–382, 1992.
36. Boothroyd, A. I., Sackmann, I.-J., and Wasserburg, G. J., *ApJ* **430**, L77–L80, 1994.
37. Boothroyd, A. I. and Sackmann, I.-J., *ApJ*, submitted.
38. Timmes, F. X., Woosley, S. E., and Weaver, T. A., *ApJ* **98**, 617–658, 1995.
39. El Eid, M., *A&A* **285**, 915–928, 1994.
40. Blackmon, J. C., Champagne, A. E., Hofstee, M. A., Smith, M. S., Downing, R. G., and Lamaze, G. P., *Phys. Rev. Lett.* **74**, 2642–2645, 1995.
41. El Eid, M. F., private communication, 1996.
42. Forestini, M., Paulus, G., and Arnould, M., *A&A* **252**, 597–604, 1991.
43. Gallino, R., Raiteri, C. M., Busso, M., and Matteucci, F., *ApJ* **430**, 858–869, 1994.
44. Boothroyd, A. I. and Sackmann, I.-J., *ApJ* **328**, 653–670, 1988.

45. Iben, I. J. and Renzini, A., *ApJ* **263**, L23–L27, 1983.
46. Schaller, G., Schaerer, D., Meynet, G., and Maeder, A., *Astron. Astrophys. Supp.* **96**, 269–331, 1992.
47. Woosley, S. E. and Weaver, T. A., *ApJS* **101**, 181–235, 1995.
48. Cameron, A. G. W. and Fowler, W. A., *ApJ* **164**, 111, 1971.
49. Boothroyd, A. I., Sackmann, I.-J., and Wasserburg, G. J., *ApJ* **442**, L21–L24, 1995.
50. Frost, C. A. and Lattanzio, J. C., "AGB stars: What should be done?", In *Proceedings of the 32nd Liége Int. Astrophys. Coll.*, edited by A. Noels, D. Fraipont-Caro, M. Gabriel, N. Grevesse, and P. Demarque. Universitè de Liége, Liége, Belgium, 1996, pp. 307–325.
51. Wasserburg, G. J., Boothroyd, A. I., and Sackmann, I.-J., *ApJ* **447**, L37–L40, 1995.
52. Charbonnel, C., *A&A* **282**, 811–820, 1994.
53. Kraft, R. P., *PASP* **106**, 553–565, 1994.
54. Langer, G. E. and Hoffman, R. D., *PASP* **107**, 1177–1182, 1995.
55. Denissenkov, P. A. and Weiss, A., *A&A* **308**, 773–784, 1996.
56. Arnould, M., Meynet, G., and Paulus, G., this volume.
57. Gehrz, R. D., "Sources of stardust in the galaxy", In *Interstellar Dust*, edited by L. J. Allamandola and A. G. G. Tielens, Dordrecht: Kluwer Academic Publishers, pp. 445–453. 1989.
58. Mowlavi, N., private communication.
59. Gallino, R., Busso, M., Picchio, G., and Raiteri, C. M., *Nature* **348**, 298–302, 1990.
60. Clayton, D. D., *ApJ* **334**, 191–195, 1988.
61. Woosley, S. E., "Nucleosynthesis and stellar evolution", In *Nucleosynthesis and Chemical Evolution*, edited by B. Hauck, A. Maeder, and G. Meynet. Geneva: Observatoire de Genéve, 1986, pp. 1–195.
62. Politano, M., Starrfield, S., Truran, J. W., Weiss, A., and Sparks, W. M., *ApJ* **448**, 807–821, 1995.
63. Meyer, B. S., Weaver, T. A., and Woosley, S. E., *Meteoritics* **30**, 325–334, 1995.
64. Colgan, S. W. J., Haas, M. R., Frickson, E. F., and Lord, S. D., *ApJ* **427**, 874–888, 1994.
65. Edvardsson, B., Anderson, J., Gustaffson, B., Lambert, D. L., Nissen, P. E., and Tomkin, J., *A&A* **275**, 101–152, 1993.
66. Prantzos, N., Aubert, O., and Audouze, J., *A&A* **309**, 760–774, 1996.
67. Mathews, G. J., Bazan, G., and Cowan, J. J., *ApJ* **391**, 719–735, 1992.
68. Penzias, A. A., *ApJ* **249**, 518–523, 1981.
69. Wilson, T. L. and Rood, R. T., *ARA&A* **32**, 191–226, 1994.
70. Henkel, C., Wilson, T. L., Langer, N., Chin, Y.-N., and Mauersberger, R., "Interstellar CNO isotope ratios", In *The structure and content of molecular clouds*, edited by T. L. Wilson and K. J. Johnston. Berlin: Springer-Verlag, 1995, p. 72.
71. Wielen, R., Fuchs, B., and Dettbarn, C., *A&A* **314**, 438–447, 1996.
72. Clayton, D. D., *ApJ*, submitted.
73. Huss, G. R., Fahey, A. J., and Wasserburg, G. J., *Lunar Planet. Sci.* **26**, 643–644, 1995.
74. Alexander, C. M. O'D., *Geochim. Cosmochim. Acta* **57**, 2869–2888, 1993.
75. Hoppe, P., Amari, S., Zinner, E., Ireland, T., and Lewis, R. S., *ApJ* **430**, 870–890,

1994.
76. Timmes, F. X. and Clayton, D. D., *ApJ* **472**, 723–741, 1996.
77. Bernatowicz, T. J., Cowsik, R., Gibbons, P. C., Lodders, K., Fegley Jr., B., Amari, S., and Lewis, R. S., *ApJ* **472**, 760–782, 1996.
78. Renzini, A. and Voli, M., *A&A* **94**, 175–193, 1981.
79. Jura, M., *ApJ* **472**, 806–811, 1996.
80. Jura, M., *ApJ* **434**, 713–718, 1994.
81. Amari, S. and Zinner, E., this volume.
82. Nittler, L. R., Hoppe, P., Alexander, C. M. O'D., Amari, S., Eberhardt, P., Gao, X., Lewis, R. S., Strebel, R., Walker, R. M., and Zinner, E., *ApJ* **453**, L25–L28, 1995.
83. Nittler, L. R., Amari, S., Zinner, E., Woosley, S. E., and Lewis, R. S., *ApJ* **462**, L31–L34, 1996.
84. Kozasa, T., Hasegawa, H., and Nomoto, K., *A&A* **249**, 474–482, 1991.
85. Clayton, R. N., Grossman, L., and Mayeda, T. K., *Science* **182**, 485–488, 1973.
86. Clayton, D. D., *Icarus* **32**, 255–269, 1977.
87. Clayton, R. N., *Ann. Rev. Earth Planet. Sci.* **21**, 115–149, 1993.
88. Thiemens, M. H. and Heidenreich, J. E., *Science* **219**, 1073–1075, 1983.